Drop Counter

Testing the performance of a simple acoustic disdrometer to measure rainfall

Abstract:

For water management in general it is of high importance to know where, when an how much rain will fall. Especially in urban areas, where water management is of more economic and social import, it is hard to measure the rainfall due to a lack of measurements at the ground. In order to provide a dense gauge network, the sensors need to be reliable, cheap and easy to maintain. The intervalometer aims to provide in this demand. Following (Uijlenhoet and Stricker 1999), all rainfall related parameters can be tight together using one parameter Λ (mm^{-1}), which characterizes the raindrop size distribution (DSD). This parameter can subsequently be related to the raindrop arrival rate $\rho_A(m^{-2} \cdot s^{-1})$ at a surface A (m^2). An extra parameter μ suggested by (Ulbrich, 1983) is implemented to determine the shape of the DSD. The raindrop arrival rate can be measured by registering the intervals between the drops hitting a piezo element. The concept of the Intervalometer is tested by using data acquired in Bago, Myanamar (monsoon season) and at the KNMI in de Bilt (the Netherlands). The DSD, the rain rate and the rain depth are calibrated and validated with respect to other rain gauges present (e.g. disdrometer, floating gauge). It is assessed that the validation sets of the rain rate and rain depth show a high coefficient of correlation of respectively $R^2 > 0.75$ and $R^2 > 0.98$. In addition, the results show a discrepancy in rain depth between 1.8% and 9.1% with respect to a reference gauge over a period of two weeks. The low costs, the simplicity and the performance of the intervalometer show a high potential for providing a dense rain gauge network in areas where there is a high demand.

Utrecht University

TU Delft

AUTHOR: JAN JAAP PAPE

UNDER GUIDANCE OF

TU DELFT:

NICK VAN DE GIESEN

MARTINE RUTTEN

UTRECHT UNIVERSITY:

MARC BIERKENS

ITC BAGO:

SAI WUNNA

CONTACT:

TU Delft

Gebouw 23
Stevinweg 1
2628 CN Delft
The Netherlands
Tel: + 31 15 27 89802

Utrecht University

Heidelberglaan 2
Room ZON 128
3584 CS UTRECHT
The Netherlands
Tel: +31 30 253 2749

Irrigation Technology Centre (ITC)

Irrigation and Water Utilization Management Department
Bago, Myanmar.
+95 9 2101087,
(or) 09 952101087 (MM)

Table of Contents

1 Introduction

Introduction to measuring rainfall and the potential of a disdrometer

1.1 Why measure rainfall?

For water management in general it is of great import to know when, where and how much precipitation will fall. For some applications an estimation of the amount of rain in an area might be sufficient. However, in other applications such as forecasting a high spatial and temporal resolution is required. Whereas the data from radars and satellites is being used increasingly, point measurements with ground gauges are still widely used as well. Either to calibrate and validate the radar data or as the main source in areas with no radar coverage(Girons lopez *et al.*, 2015). The potential of point measurements to provide high spatial resolution is highly dependent on the number, location and reliability of the weather stations.

In order to provide adequate flood warning systems the World Meteorological Organisation (WMO) provided guidelines for the minimum rain gauge densities(Rodda, 2011). However, the lack of coverage and unsustainable gauge networks continues to be the main problem regarding the provision of high resolution rain data. In addition, all the WMO approved rain gauges are in rural areas in order to meet the WMO requirements. Therefore it is hard to acquire high resolution rain data in urban areas, whereas the water management in urban areas is of more economic and social import. Impermeable pavements and a lack of green causes local flooding because the water is not able to drain quick enough. In order to provide adequate solutions it is important to map the variability of the rain intensity in the city and hence to increase the rain gauge network (KNMI, no date; Rodda, 2011).

1.2 Current methods

Over the years a lot of methods to measure precipitation have been developed. The WMO distinguishes a couple of methods for rain gauges which are described in the next sections. Note that there are more methods available but not yet widely used. Examples can be found in crowdsourced measurements or by making use of the distortion between satellite links caused by raindrops (Muller *et al.*, 2015; van het Schip *et al.*, 2017).

1.2.1 Weighing recording gauge

This is one of the most simple methods to record the amount of rain which has fallen in a certain time period. The precipitation is collected in a bucket and its weight can be converted to the amount of rain. The benefit is that it is easy to measure other types of precipitation like snow or hail because it is not required to melt the precipitation first. However, in order to empty the bucket a set of levers and moving elements is required. In addition, these types of gauges are sensitive to errors caused by evaporation losses and the influence of strong winds, animals or rubble getting into the bucket (Rodda, 2011).

1.2.2 Float Gauge

An alternative instrument is the float gauge, where the water level in a bucket is monitored by a floating element. A heating element needs to be installed in order to guarantee that the precipitation is in liquid form and to prevent freezing of the floating element. The emptying of the bucket can then be realized by a siphoning process. The disadvantage is that the heating element increases the potential losses caused by evaporation (Rodda, 2011).

1.2.3 Tipping bucket

The principle of this rain gauge is based on two light metal containers which are connected on a horizontal axis. After a small amount of rain has fallen into one container, the axis becomes unstable, tips over and the water flows out of the container. The rain can then fall in the other container which is now in its upper position. The advantages of this gauge are that the signals can easily be automated and registered at a distance. The disadvantage is that the precipitation is discretely registered, so the beginning and end of a light rain event cannot be determined accurately. In addition, the error due to evaporation losses during light rain events are enhanced because of a relatively large water surface (Rodda, 2011).

1.2.4 Disdrometer

A disdrometer measures the amount and size of precipitation particles. This can be done be measuring the impact of drops on a sensor surface, like with the Delft Disdrometer (Hut *et al.*, 2013) or by measuring the reflectivity of drops when illuminated with microwaves. The advantage of this method is that the drop size distribution (DSD) is also registered. The drop size distribution ties all the rainfall related parameters together and is therefore better suitable as a ground source to calibrate satellite data (Uijlenhoet and Stricker, 1999). The disadvantage is that the current disdrometers are relatively expensive which prevents the spreading of a dense gauge network (Rodda, 2011).

Since the disdrometer measures the DSD which ties all rainfall related parameters together, this type of gauge is preferred over the other rain gauges. Previous research has been done on providing a cheap disdrometer by making using a piezo element to register the impact of the raindrops (Hut *et al.*, 2013; Honingh, 2016). This Delft disdrometer measures the DSD directly by assuming a relationship between the amplitude of an incoming signal and the drop size. However, research has shown that the Delft disdrometer yields some problems regarding the calibration (Honingh, 2016).

1.3 Drop Counter (Intervalometer)

In order to provide high spatial resolution data and provide adequate solutions for the problems which occur with intense rainfall a dense gauge network is required. To provide a dense gauge network, the sensors need to be reliable, cheap and easy to maintain. These requirements are used as a reference for the development for a new rain gauge; the Drop Counter.

1.3.1 Concept

To prevent problems regarding the calibration, another method to determine the DSD is suggested by making use of the Drop Counter. Following Uijlenhoet and Stricker (Uijlenhoet and Stricker, 1999), the DSD can be simulated by making use of one parameter $\Lambda\ (mm^{-1})$, which characterizes the raindrop size distribution. This parameter can subsequently be related to the raindrop arrival rate $\rho_A(m^{-2} \cdot s^{-1})$ at a surface $A\ (m^2)$. The raindrop arrival rate can be measured by simple counting the number of drops hitting a piezo element. The piezo is placed on a 3D printed holder and the signal is processed by an Arduino datalogger. This is an easy to use and well documented datalogger which is becoming more popular in science projects (Mesas-Carrascosa *et al.*, 2015). In order to support the reliability of the data, the intervals between the drops is registered as well. By keeping it simple, the problems regarding the calibration are aimed to be restricted to a minimum.

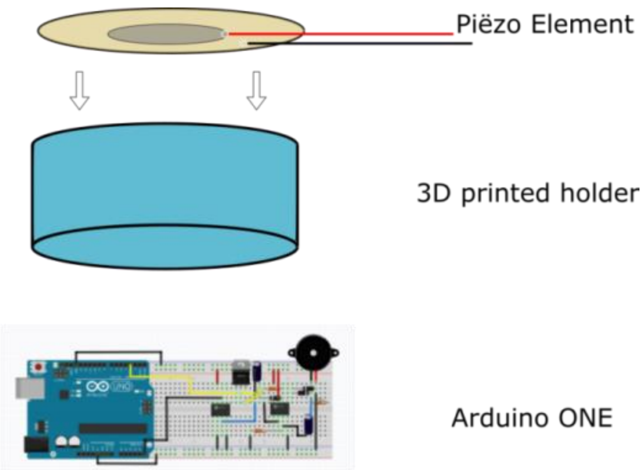

Figure 1: The elements used in the concept of the Drop Counter

1.3.2 Aims

The aim of this report is to show the potential of a simple disdrometer with a piezoelectric disk as a sensor called the Drop Counter. The Drop Counter has to comply to three conditions:

- It has to be simple, so that hobby meteorologists are able to make their own sensor.
- It is made of materials which are readily available worldwide for a low price.
- It will provide the user with some useful data regarding rain related parameters.

1.3.3 Research questions

To what extent the Drop Counter is providing reliable data compared to current techniques is still to be investigated. Hence the research questions are:

- How accurate can the Drop Counter measure the rain intensity?
- How accurate can the cumulative rainfall be presented by the Drop Counter compared to other rain gauges?
- Do the DSD’s estimated by the Drop Counter correspond to the DSD’s measured by another rain gauge?

2 Drop Counter

Description of the design and concept of the Drop Counter

2.1 Design concept

The design of the Drop Counter is also kept simple. A piezo element is placed on top of a 3D printed holder and connected to an Arduino board. The holder is placed on top of a kitchen sponge to limit the noise from outside which can trigger the sensor and give rise to false readings. To protect the piezo element, the disk is covered with hydrophobic material which can be car spray, nail polish or any other hydrophobic alternative. The wiring is guided through a PVC pipe to support the sensor and keep the piezo in a parallel position with respect to the ground. When the sensor is triggered, the signal goes to the Arduino board, where the intervals are stored on a SD card. To keep the Arduino board dry, the datalogger is placed inside a logger box with three rubber-sealed inputs; one for the power supply, one for the signal from the piezo and another one for a check-LED. The PVC pipe with the sensor can either be fixed to the logger box with cloth tape or fixed in the ground with skewers. For convenience a LED can be fixed to the exterior of the sensor to be able to check whether the Drop Counter is functioning properly. The conceptual design can be observed in Figure 2.

Figure 2: Conceptual design of the Drop Counter

2.2 Logging the signals

When a drop hits the piezo element, the deformation of the metal disk will cause a small potential difference between the plus and minus outputs from the piezo. This signal is processed and stored by using an Arduino datalogger. Arduino boards are well documented and easy to use for hobby meteorologists. The basic knock sensor by Arduino is used as an example for the design of the Drop Counter datalogger (*Arduino - Knock sensor*, no date). Note that in the development of the Drop Counter different schemes and their effect on the performance of the Drop Counter have been investigated. The results of these test are presented in a logbook which is kept during the measurements (Pape, 2018). It appeared that a scheme similar to the knock sensor example with an added shortcut leads to the best results.

In the knock sensor example by Arduino the plus output is connected to an analogue pin and the minus to the ground of the Arduino (Figure 3A). The plus and minus are connected with a large pull-down resistor to prevent floating pins and consequently false readings at the analogue pin. After a drop has hit the sensor, the disk should stop vibrating as quick as possible in order to prevent double readings from one drop and interference between two drops. To realize this, a shortcut is added to the circuit so that the piezo element is put to rest position after a signal has been detected at the analogue pin by supplying a 'high'-signal at Pin6 (Figure 3B).

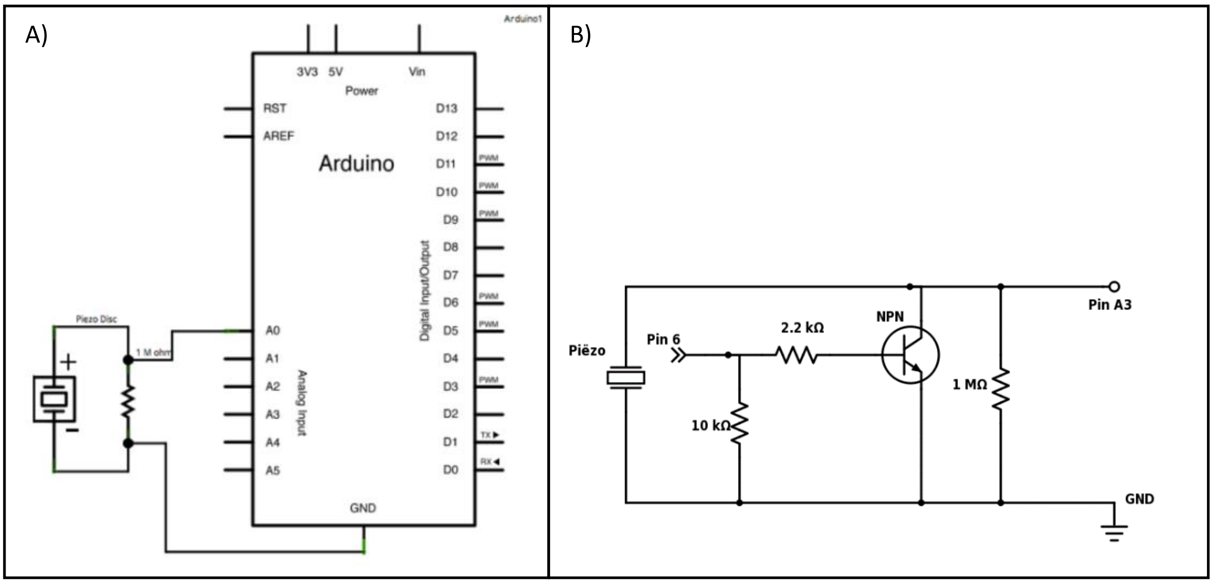

Figure 3: A) schematic visualization of the knock sensor example by Arduino (*Arduino - Knock sensor*, no date). B) Schematic visualization of the circuit used in the Drop Counter.

When a signal is received at Pin A3, the time interval (ms) between the signal and the previous one is logged on an SD card. This is done by making use of an Adafruit assembled data logging shield. To be able to know when the logger was last alive, the logger also writes the UNIX time on the SD card with an interval of 30 seconds. Another check is realized by fixing an LED to one of the digital pins, which will blink if there is a signal received at the analogue pin. The LED is guided through one of the inputs of the logger box so that the logging of the signals is still visible when the logger is in the logger box.

2.2.1 Threshold

An important thing to note is that a signal has a certain amplitude which can correspond to a drop hitting the sensor. However, due to background noises the piezo element will produce low amplitude signals all the time. An amplitude threshold is implemented to guarantee that the piezo is triggered by a drop and not by background noises. The threshold is included in the Arduino code, which can be found in the Logbook (Pape, 2018). Note that the detection threshold for the Arduino board is smaller than the amplitudes of noisy signals, so no amplification of the signals from the drops is required (Pape, 2018).

2.2.2 Range of raindrops

Whereas false positives are prevented through an amplitude threshold, some low amplitude signals from small raindrops may also be neglected. Since the Drop Counter aims to register the DSD it is important to know what the minimum raindrop sizes are which can still be detected. This is investigated by performing a simple test with an electro valve and a syringe needle, which is able to produce very small drops. The drops are produced by pushing the water through an electro valve which can be opened and closed with a temporal accuracy of 1ms. The drop sizes can consequently be varied by applying different amounts of water to the valve, regulated by the open time of the valve. At the end of the electro valve a needle is fixed to realize small spherical drops. The experimental setup is visualized in Figure 4.

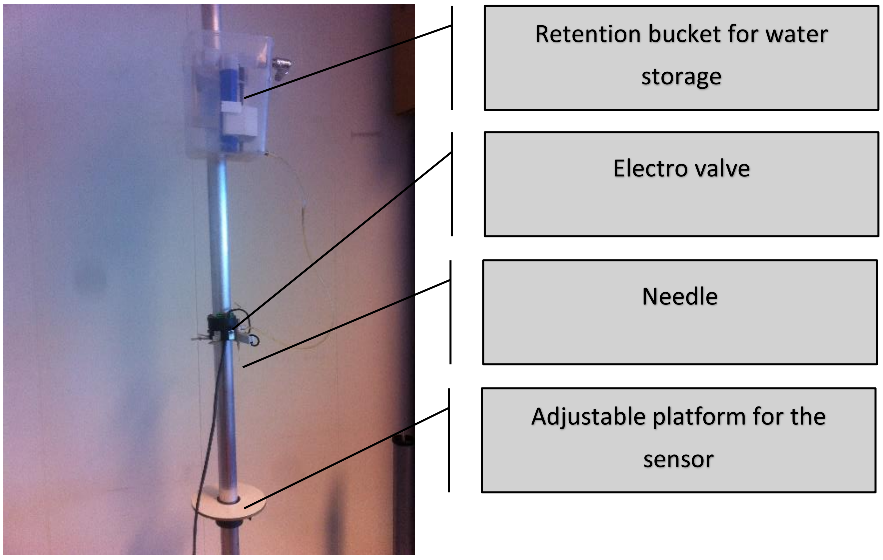

Figure 4: Experimental setup to assess the range of detectable raindrops.

Note that the electro valve is limited to produce drops down to 1.93mm in diameter, whereas raindrops can range down to lower than 0.5mm in diameter. Since there is a limit to the drop sizes which can be produced with the electro valve, the fall height is decreased in small steps in order to get an idea of the minimum energy which can be registered with the Drop Counter. The energy of the drops is calculated by assuming a drag force working on a perfect sphere falling through air. Consequently, the minimum energy is linked to a minimum drop size.

The test is only performed with one Drop Counter. The results are not very stable, because of two reasons. Firstly a puddle of water forming on the sensor can damp the impact from a drop. Secondly the edges of the sensor are stiffer than the centre of the sensor, which causes more divergent results. This effect is previously described by (Honingh, 2016). However repetitive experiments show that a minimum detectable drops diameters of approximately 1.0mm can be used as a standard for the Drop Counter. In theory there should be no maximum detectable drop size (Pape, 2018).

2.2.3 Filter

To further prevent the influence of noisy signals a digital filter is implied to filter out any other noise caused by an electromagnetic field (EMF) or unknown sources. This is based on the following concept. When a drop hits the sensor, the piezo disk will start to vibrate with a certain frequency which corresponds with the frequency registered at the analogue pin. Other signals like radio frequency interference will cause a signal with a much higher frequency which will be filtered out by the digital filter. The digital filter only passes a range of frequencies between 10 and 2000 Hz, which is empirically determined with testing the performance of the Drop Counter (Pape, 2018).

2.3 Materials and cost

In Table 1, the bill of materials can be found. As formulated in the aims section, the materials used are relatively cheap. All materials can be ordered online and shipped to any location demanded. For the steps made in the assembly of the Drop Counter a reference further reading in the Logbook is recommended (Pape, 2018).

Table 1: Bill of materials

Item	Price	Number	Remarks	Subtotal
Arduino UNO	$ 23.38	1		$ 23.38
Data cable	$ 2.07	1		$ 2.07
Adafruit Data Logging Shield	$ 13.95	1		$ 13.95
Screw terminals	$ 0.57	1	(price at ten pieces)	$ 0.57
Jumper wires	€ 18.36	0		$ 21.70
Pull down resistors 2200 Ohm	€ 42.16	0	kit for all resistors, 100 each	$ 49.83
Pull down resistor 1 10kOhm				$ -
Pull down resistor 2 1MOhm				$ -
Transistor 2N5551	€ 0.15	5		$ 0.86
Zener diodes 3V	$ 0.14	1		$ 0.14
Mosfet BS170	$ 0.48	2		$ 0.96
			Total	$ 113.46
		Fixed costs wires and resistors		$ 73.60
		Price per meter		$ 39.86

3 Sites & Methods

Description of the data and methods used to test the performance of the Drop Counter.

3.1 Sites

Datasets were obtained at three different locations. At each location, different rain gauges were available for calibrating and validating the drop counter. An overview of the availability of rain gauges at each location is presented in Table 2.

3.1.1 Bago, Myanmar

The first data were collected at the Irrigation Technology Centre (ITC) in Bago, Myanmar. This region is classified as a tropical monsoon climate, where a high chance of high rain intensities is found in the monsoon season (Kottek *et al.*, 2006). Since the smallest drop sizes are not registered by the Drop Counter, it was expected to estimate the rain rates more accurately with high rain intensities. Therefore this location was well suitable for testing the Drop Counter.

At the measure field of ITC two Delft disdrometers 2.0, a tipping bucket and a manually registered daily sum gauge were available. One Drop Counter was placed at the measure field and one was placed approximately 100m from the measure field. Due to malfunctioning in the dataloggers from the disdrometers and the tipping bucket, some of the data of the disdrometer were not useful. In addition, no data were registered by the tipping bucket during the time of measurement. The useful data for each rain gauge can be observed in Table 2.

3.1.2 Delft, the Netherlands

The second dataset was obtained in Delft, the Netherlands has a temperate oceanic climate (Kottek *et al.*, 2006). At this location another Delft disdrometer and a tipping bucket were available for calibration and validation. The measurements started at 18/12/2017 and ended at 31/01/2018. However, due to storm damage to the power supply all useable data were lost. Hence, no results could be presented from this site.

3.1.3 KNMI de Bilt, the Netherlands

A third set was obtained at the site of the Royal Dutch Meteorological institute in de Bilt, which has a temperate oceanic climate (Kottek *et al.*, 2006). A floating gauge was chosen as a reference set for the Drop Counter. Since the precipitation gauge from the KNMI is WMO registered, the results were expected to show a better representation of reality with respect to the Delft disdrometers. The measurements were taken from 20/12/2017 to 31/01/2018. Due to very strong winds the sensor was blown out the PVC pipe which made the data from 22/12/2017 until 03/01/2018 unreliable. On top of that, the sensor failed because of water damage from 23/01/2018 until the end of the dataset.

Table 2: Rain gauges availability

Sensor ID	Gauge type	Location	Data period	Notes
DC 1	Drop Counter	ITC, Bago, MYM 100m from measure field	12/10/2017 - 26/10/2017	
DC 2	Drop Counter	ITC Bago, MYM measure field	12/10/2017 - 26/10/2017	
Z03	Delft Disdrometer	ITC, Bago, MYM measure field	18/10/2017 - 26/10/2017	
Z04	Delft Disdrometer	ITC, Bago, MYM measure field	12/10/2017 - 26/10/2017	
TIP 1	Tipping Bucket	ITC, Bago, MYM measure field	NA	Failed due to technical problems
MAN 1	Manual bucket gauge	ITC, Bago, MYM measure field	01/01/2017 - 31/10/2017	Reports of Daily sum
DC 1	Drop Counter	KNMI, De Bilt, NLD	20/12/2017 - 31/01/2018	Data missing due to storm and water damage
DC 2	Drop Counter	YES!Delft, Delft, NLD	18/12/2017 - 31/01/2018	Full dataset missing due to storm damage
KNMI 1	Float gauge	KNMI, De Bilt, NLD	20/12/2017 - 31/01/2018	Data not validated
Z05	Delft Disdrometer	YES!Delft, Delft, NLD	18/12/2017 - 31/01/2018	Full dataset missing due to storm damage

3.2 Methods

In order to present a robust perspective on the performance of the Drop Counter and answer the research questions, the following methods are used:

- The rain rates estimated by the Drop Counter are compared to the rain rates of other available rain gauges (e.g. tipping bucket or disdrometer) .
- The cumulative rainfall estimated by the Drop Counter is compared to the rain depth of other rain gauges.
- The theoretical DSD estimated by the Drop Counter is compared to the measured DSD by the disdrometers.

3.2.1 From arrival rate to rain rate

To be able to compare the results of the Drop Counter to other rain gauges, the number of drops per time unit need to be converted to the DSD or the rain rate. Uijlenhoet and Stricker (Uijlenhoet and Stricker, 1999), showed that the DSD can be simulated by making use of one parameter Λ (mm^{-1}), which characterizes the raindrop size distribution. They showed that the raindrop size distribution $N_V(D)$ for rain rates between 1 and 23 mm·h^{-1} can be described by a simple negative exponential parametrization (Marshall *et al.*, 1948):

$$N_V(D) = N_0 \exp(-\Lambda \cdot D) \quad (1)$$

Where $N_V(D)$ is the expected number of raindrops between D and dD (mm) per unit volme of air (m^3), $N_0 = N_V(0)$ is the intercept which appeared to be constant for all rain intensities at about 8000 and Λ decreased with increasing rain rate R as a power law $\Lambda = 4.1 \cdot R^{-0.21}$. However, Ulbrich (1983) (Ulbrich, 1983) showed that further accuracy can be achieved if the DSD is assumed to be a gamma distribution of the form:

$$N_V(D) = N_0 \mathrm{D}^{\mu} \exp(-\Lambda \cdot D) \quad (2)$$

Where μ can have any positive or negative value and determines the shape of the DSD. Note that an additional parameter is used, so à priori knowledge concerning a relationship between two of the parameters is required to use this method in measurement techniques. In order to simulate the raindrop arrival process, it is assumed that $N_A(D) = v(D)N(D)$, where $v(D)(m\ s^{-1})$ denotes the terminal fall speed of a raindrop with diameter D (cm) in still air, thus neglecting the impact of wind and turbulence. The expected number of raindrops $N_A(D)$ with sizes between D and dD (mm) arriving at a surface $A\ (m^2)$ per time unit $T\ (s)$ can then be expressed as:

$$N_A(D) = \alpha \cdot N_0 D^{(\beta+\mu)} \exp(-\Lambda \cdot D) \tag{3}$$

Where $\alpha(m\ s^{-1})$ and $\beta\ (-)$ are parameters in $v(D) = \alpha \cdot D^{\beta}$ and are estimated to be respectively $3.778 \cdot 10^{-\beta}$ and 0.67. N_0 is described by an empirical relationship $N_0 = 6.0 \cdot 10^4 \exp(3.2\mu)$ assessed by (Ulbrich, 1983). Integrating $N_A(D)$ with respect to D between 0 and ∞ leads to an expression for the arrival rate $\rho_A\ (m^{-2}s^{-1})$:

$$\rho_A = \int_0^{\infty} N_A(D)dD = \alpha \cdot N_0 \cdot \frac{\Gamma(1+\beta+\mu)}{\Lambda^{1+\beta+\mu}} \quad and \quad \Lambda = \left(\frac{\alpha N_0}{\rho_A} \cdot \Gamma(1+\beta+\mu)\right)^{\frac{1}{1+\beta+\mu}} \tag{4}$$

The rain rate R can subsequently be derived by using the theoretical relation $D_0 = \epsilon R^{\delta}$ where $\epsilon = (3.67 + \mu)(33.31 N_0 \Gamma(1 + 3.67 + \mu)^{-\frac{1}{1+3.67+\mu}}$, $\delta = \frac{1}{1+3.67+\mu}$ and $D_0\ (cm)$ is the median volume diameter (Ulbrich, 1983). If $D_0/D_{max} \geq 2.5$, it can also be assumed that $\Lambda D_0 = 3.67 + \mu$ and the following expressing for R is obtained:

$$R = \left(\frac{3.67+\mu}{\epsilon\Lambda}\right)^{\frac{1}{\delta}} \tag{5}$$

Since the arrival rate is registered by the Drop Counter, the rain rate R can be determined using equation (2), (4) and (5). The DSD is assessed, using the probability density function which represents the probability of diameter D(cm) with a given Λ value:

$$f_{D_A}(D) = \rho_A^{-1} N_A(D) = \frac{\Lambda^{1+\beta+\mu}}{\Gamma(1+\beta+\mu)} \cdot D^{\beta+\mu} \exp(-\Lambda \cdot D) = \frac{\alpha N_0}{\rho_A} \cdot D^{\beta+\mu} \exp(-\Lambda \cdot D) \tag{6}$$

In Figure 5 the probability density function is shown for three rain intensities and corresponding $\Lambda\ (\mu = 0)$ values. Note that as expected there is a higher probability of small drops with low rain intensities and vice versa.

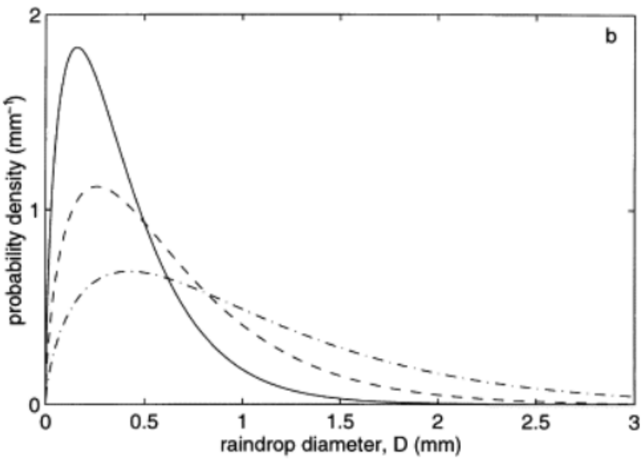

Figure 5: probabiliy density function of drop diameters D arriving at a surfaca A per time unit T, for rain rates: 1mm/h (solid line), 10mm/h (dashed line) and 100mm/h (dashed-dotted line) (Uijlenhoet and Stricker, 1999).

3.2.2 Comparing rain intensity and rain depth

First the rain rates and the cumulative rain rate will be calibrated and validated with respect to a reference rain gauge. This is done by making use of equation (1-6). A moving window technique is used to present the data from the Drop Counter and a reference dataset in the same timeframe and units. This means that at each time interval Δt a statistical analysis is performed on the Drop Counter data and the rain related parameters are calculated. The rain related parameters from the reference dataset are calculated as well and scaled with respect to the window length Δt. The start and ending date and time T_0, T_e are predefined so that each timeframe is identical for the Drop Counter data and the reference set. The effect of Δt on the performance of the Drop Counter is tested as well.

3.2.2.1 Calibration and validation

Apart from the variations in the sensors and the assembly of the sensors, the fact that μ has to be estimated demands for calibration of the data. In addition, some of the assumptions in equations (2-6) are not valid in practice. Therefore the data is calibrated by making use of a reference set from another rain gauge. This is done by using μ as a calibration coefficient. Consequently μ is optimized so that the root mean square error (RMSE, eq 7) calculated from the rain intensities of the two datasets is smallest. For the optimizing the RMSE, Brent's method for root finding is used and μ is limited to $\mu \in (-2{,}25)$ (Brent, 2013). Both the calibration and the validation set are preferred to be of a minimal length of one week. To prevent any prejudice concerning the validation set, the calibration set is always the first half of the total dataset and can never be longer than the validation set.

$$RMSE = \sqrt{\sum_{i=1}^{N} \frac{(x_i - y_i)^2}{N}} \qquad (7)$$

3.2.2.2 Sensitivity analysis C_{N_0}

Since some of the relations in equation (2-6) are based on experimental data, it is assessed whether the results of the Drop Counter with respect to a reference gauge can be improved. This is done by performing a sensitivity analysis on the coefficientC_{N_0} in $N_0 = C_{N_0} \exp(C_\mu \cdot \mu)$, with $C_\mu = 3.14$. In the work of (Ulbrich, 1983) two values are suggested for C_{N_0} (i.e. 1.52e^4 and 6.0e^4), where the discrepancy between the two values was not explained. Therefore it is assessed whether adjusting C_{N_0} will lead to improved results regarding the calibration and validation.

3.2.2.3 Maximum arrival rate and minimum number of drops

Two methods are suggested to limit the effect of errors caused by EMF or other external sources of noise. Firstly a maximum arrival rate is implied. When the arrival rate is exceeding realistic values, that specific precipitation event is no longer taken into consideration. Realistic values are defined as arrival rates up to 8 drops per second. Experimental data, like the example output in Figure 6 leading to an arrival rate of ≈ 8.5 drops/second, has shown that arrival rates faster than this are indicating a noisy signal. Secondly a minimum number of drops per rain event is implied. This will guarantee that the rain event has enough data to perform a statistical analysis, like calculating the DSD. The minimum amount of raindrops necessary to perform an analysis is assessed to be 10 drops. These two methods will reduce the chance of registering noise as a raindrop. E.g. electromagnetic interference will cause constant triggering of the analogue pin which will lead to unrealistic rain rates. The disadvantage is that useful data might be lost as well.

Figure 6: Example of serial output from Drop Counter; output value(0 - 1024, which scales to an analogue value of 0 - 5V) printed on first lines, interval (ms) printed on each second line.

3.2.3 Reclass rain intensity

The estimated rain intensities from the Drop Counter can yield relatively large errors due to the errors in the assumptions regarding the calculation of the rain intensities. In addition, not all drops are registered because there is a minimum detectable drop size (≈1.0mm). Therefore it is assessed whether the Drop Counter is better suitable to estimate the rain intensities in classes. Five classes are defined, with the following intensity I in mm/h (Llasat, 2001):

- light rainfall = $I < 2\ mm/$h
- moderate rainfall = $2 \leq I \leq 15\ mm/h$
- heavy rainfall = $15 < I \leq 30\ mm/$h
- very heavy rainfall = $30 < I \leq 60\ mm/h$
- torrential rainfall = $I > 60\ mm/h$

3.2.4 Comparing DSD

Since the Drop Counter also makes an estimate of the DSD, this parameter is compared to a reference set as well. In order to do so, the reference gauge is required to estimate the drop sizes. The disdrometers which are available at Bago (Myanmar) and in Delft (the Netherlands) are well suitable for this purpose. The probability density function derived from the results of the disdrometer is compared to the distribution estimated from the Drop Counter data (equation (6)). A kernel density estimation (KDE) is used to estimate the probability density function (PDF) from the disdrometer data. Scott's rule of thumb is used to estimate the bandwidth parameter of the KDE (Scott, 2015). In order to quantify whether the estimated distribution from the Drop Counter is coinciding with the distribution from the disdrometer the Kullback-Leibler (KL-) divergence is calculated (eq. (10)). This is defined as the expectation of the log difference between the probability of data in the original distribution with the approximating distribution (Kullback and Leibler, no date). In this case the estimated distribution from the disdrometer will be considered as the original distribution and the Drop Counter estimate as the approximating distribution. If the KL-divergence is close to 0 the pdf estimated from the Drop Counter is considered to be a good approximation and if it is bigger than 1 a bad one.

$$D_{KL}(p||q) = \sum_{i=1}^{N} p(x_i) \cdot \log\left(\frac{p(x_i)}{q(x_i)}\right) \tag{10}$$

4 Results

Results from the data obtained in Myanmar and the Netherlands

4.1 Rain intensity and rain depth

4.1.1 Bago (Myanmar)

4.1.1.1 Window length of 3 hours

The results from Z04 and one DC2 (see Table 2) are presented in Figure 7. The calibration and validation set are both approximately one week. A window length of 3 hours is set as a standard in order to present a set with sufficient data for each precipitation event. In Table 3 the statistics of the rain intensity, rain depth and the reclassed set are presented for the validation set. It is observed that the rain intensity as well as the rain depth estimated by the Drop Counter are strongly ($R^2 > 0.96$) corelated to the intensity and rain depth measured by the disdrometer. Apart from that, it is observed that high rain intensities are overestimated and low rain intensities are underestimated by the Drop Counter. In addition, the reclassed sets from the disdrometer and the Drop Counter are showing a decreased correlation with respect to the original rain intensity.

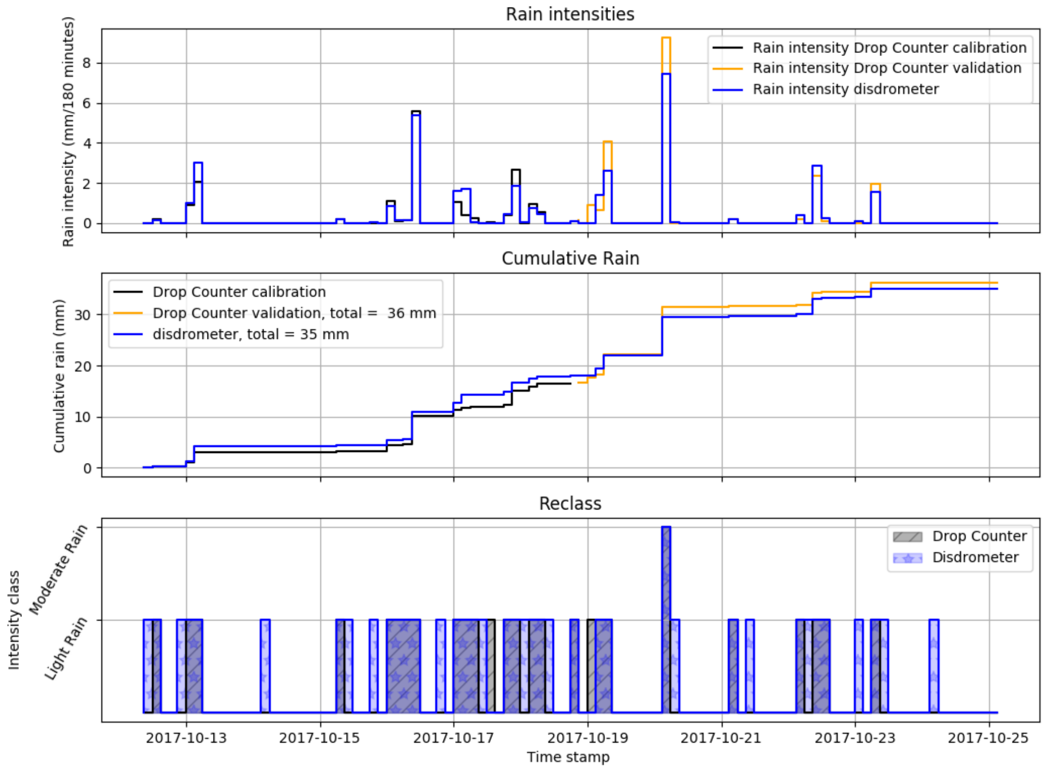

Figure 7: Results DC2and Z04 at Bago Myanmar.

Table 3: Statistics Bago, DC2 and Z04 validation set, WL = 3 hours

	Intensity	*Cumulative*	*Intensity (reclass)*
MBE (mm)	0.05	1.17	NA
RMSE (mm)	0.38	1.46	NA
R^2 (-)	0.96	0.99	0.47

4.1.1.2 Shorter window lengths

The minimum time interval (i.e. the level of detail) which can be used to determine the rain intensity with the Drop Counter is assessed by decreasing the window length. The statistics for shorter window lengths are presented in Table 4. It is observed that R^2 is decreasing for the intensity with decreasing window length. However, the R^2 for the rain depth is more or less stable with decreasing window length. In addition, the RMSE of the rain depth is decreasing with decreasing window length until WL=30 min, which shows the following effect. With a large window length the rain intensity is averaged over a larger time period and will underestimate the high rain intensities which occur in a short time period. Hence the high rain intensities are underestimated with a large window length. When WL=10 min. the MBE of the rain depth is relatively high and negative whereas it is expected to be positive because the high rain intensities can be presented in higher detail. This indicates the loss of data due to the minimum raindrops condition. Hence the maximum level of detail for this Drop Counter is assessed to be approximately 30 minutes. Note that in neither of the window lengths, reclassing the intensity leads to improved results.

Table 4: Statistics Bago, DC2 and Z04 validation set, WL = {60, 30, 10} minutes.

WL=60 min.	***Intensity***	***Cumulative***	***Intensity (reclass)***
MBE (mm)	0.02	0.70	NA
RMSE (mm)	0.21	1.13	NA
R^2 (-)	0.94	0.99	0.51
WL=30 min.			
MBE (mm)	0.01	-0.74	NA
RMSE (mm)	0.22	1.10	NA
R^2 (-)	0.76	0.99	0.42
WL=10 min.			
MBE (mm)	-0.004	-10.43	NA
RMSE (mm)	0.11	10.50	NA
R^2 (-)	0.54	0.99	0.36

4.1.1.3 Combining all datasets

Thus far only the datasets from DC2 and disdrometer Z04 were presented. As a supplement all available data from Bago Myanmar is presented in Figure 8. Both DC 1 and DC 2 are calibrated with respect to disdrometer Z04, where the first half of the presented time period is the calibration set and the second half the validation set. It is observed that disdrometer Z04 shows higher rain intensities and rain depth with respect to Z03. In addition, all the Drop Counters and disdrometers underestimate the rain depth when compared to the manual gauge MAN 1. Apart from that, a small error between DC 1 and DC 2 is observed. This shows that when two Drop Counters are calibrated with respect to the same gauge the way of assembling the Drop Counter or the used piezo element hardly influences the resulting rain intensity. This is important for the consistency of the results obtained from Drop Counters.

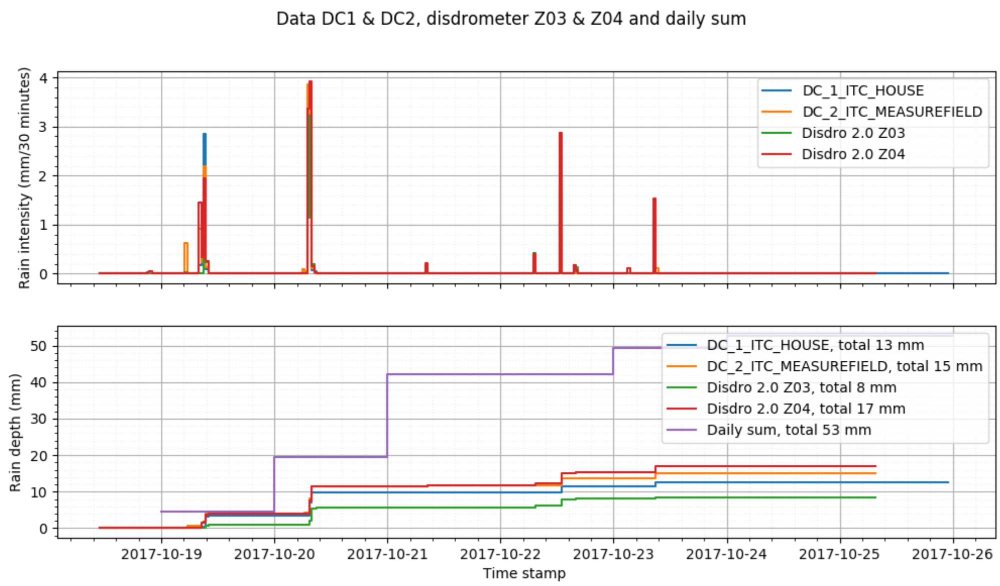

Figure 8: Figure combining all available data from Bago (Myanmar). Top: Rain intensity, Bottom: Rain depth.

4.1.2 Delft (the Netherlands)

Due to storm damage, there are no results to show from the measurements in Delft.

4.1.3 KNMI (the Netherlands)

4.1.3.1 Window length 30 minutes

Since a window length of 30 minutes is observed to lead to optimal results with the highest level of detail, this window length was set as a reference window length for the set of DC 1 and KNMI 1. In Figure 9 the results for DC 1 and KNMI 1 at the Bilt (the Netherlands) are presented. Firstly, it is observed that the dataset is longer than the dataset from Bago (Myanmar) and the rain is less frequent than in the monsoon season in Myanmar. Secondly, the maximum rain intensities are lower with respect to the observed intensities in Bago (Myanmar). Both the RMSE and coefficient of correlation of the intensity in Table 5 are significantly less than in Table 4 (WL=30). In addition, the error (RMSE) in the rain depth is much larger with respect to the set of DC 2 and Z04. Performing a reclassification of the rain intensities does not seem to improve the results or result in any additional insight either.

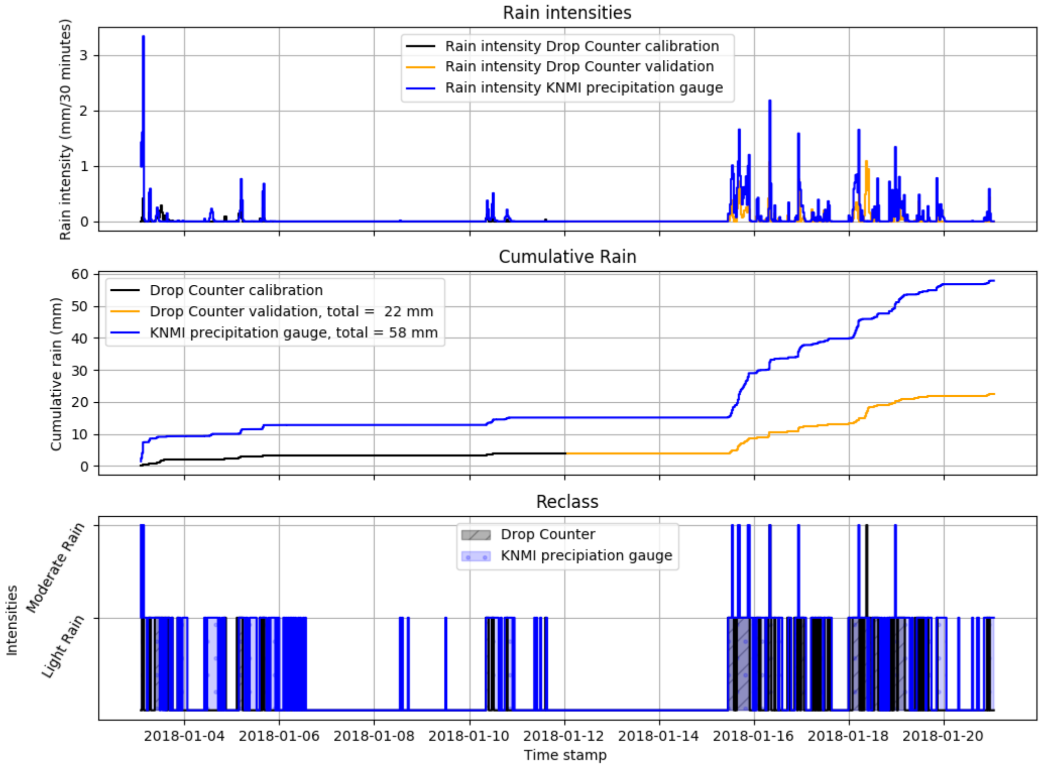

Figure 9: Results DC 1 and KNMI 1, from 03/01/2017 to 23/01/2017

Table 5: Statistics the Bilt, DC 1 and KNMI 1 validation set, WL = 30 minutes

	Intensity	*Cumulative*	*Intensity (reclass)*
MBE (mm)	-0.06	-21.53	NA
RMSE (mm)	0.20	23.45	NA
Rsqrd (-)	0.52	0.99	0.24

4.1.3.2 Sensitivity analysis C_{N_0}

Since the RMSE of the validation set of DC 1 and KNMI 1 is relatively big, a sensitivity analysis with respect to C_{N_0} is performed to check whether the results can be improved. C_{N_0} is varied in a range of C_{N_0} =1*10$^{\{0,1,\ldots,6\}}$. The statistics of the validation set with varying C_{N_0} are presented in Figure 10. Firstly, it is observed that the MBE for the intensity as well as the rain depth goes from positive to negative values for increasing C_{N_0}. This indicates that the rain intensities are estimated to be lower with increasing C_{N_0}. Secondly the RMSE of the rain depth shows a minimum at $C_{N_0} = 10$ and the RMSE for the intensity has a maximum for $C_{N_0} = 100$. Thirdly the R^2's of the intensity as well as the rain depth hardly seem to be affected by varying C_{N_0}. Except for $C_{N_0} = 100$ where the R^2 of the intensity is showing a minimum. The optimal value of C_{N_0} for this set is assessed to be $C_{N_0} = 10$.

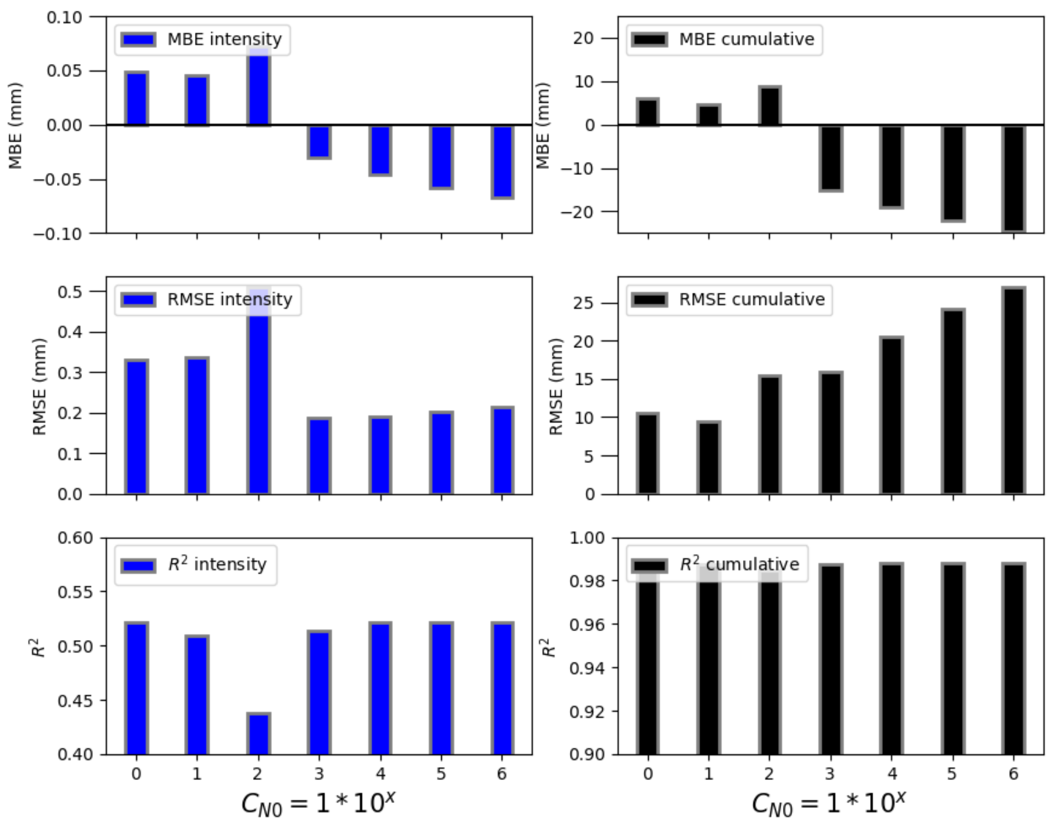

Figure 10: Results sensitivity analysis C_{N_0}, DC 1 and KNMI 1.

4.2 DSD

4.2.1 Bago (Myanmar) DC 2 and Z04

Each window length a DSD is estimated by the Drop Counter. Hence a sample window is used to compare the DSD from the Drop Counter with respect to the DSD derived from the disdrometer data. An optimal level of detail with a window length of 30 minutes is taken as a reference for the calibration. In Figure 11 the sample window is visualized by the grey shaded area. In the zoomed graph it is observed that the error in estimated rain intensity by DC 2 is relatively small compared to Z04. Hence the DSD's are expected to be similar. In Figure 12 the DSD's derived from DC 2 and Z04 in the selected period (2017/10/19 8:51 to 2017/10/19 9:22) are presented. It is observed that the mode from Z04 is smaller than the mode from DC2. In addition, the KL divergence is 1.3 cm^{-1} which is bigger than 1 and hence regarded as a bad approximation.

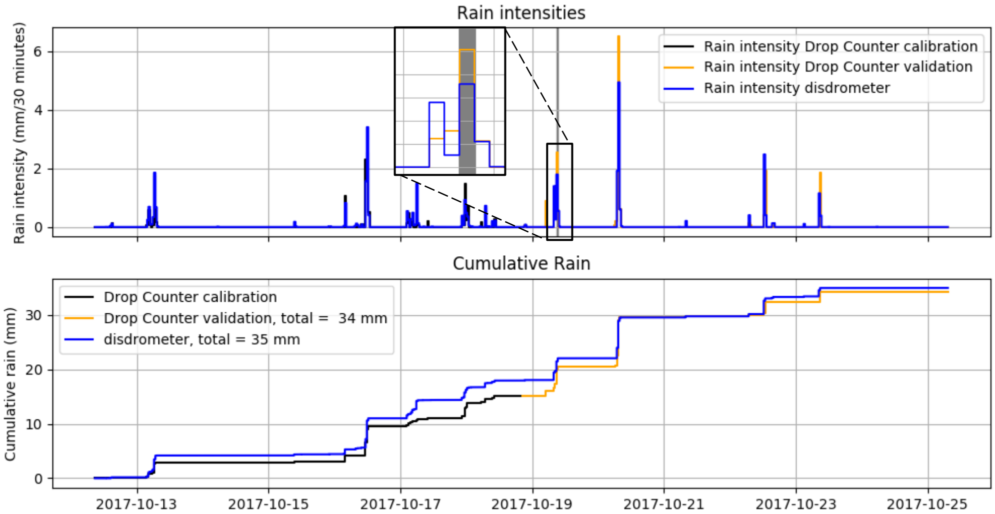

Figure 11: Results rain intensity and rain depth DC 2 and Z04, WL=30min (minimum window length). Top: Rain intensity with zoomed area of DSD selection. Bottom: Rain depth.

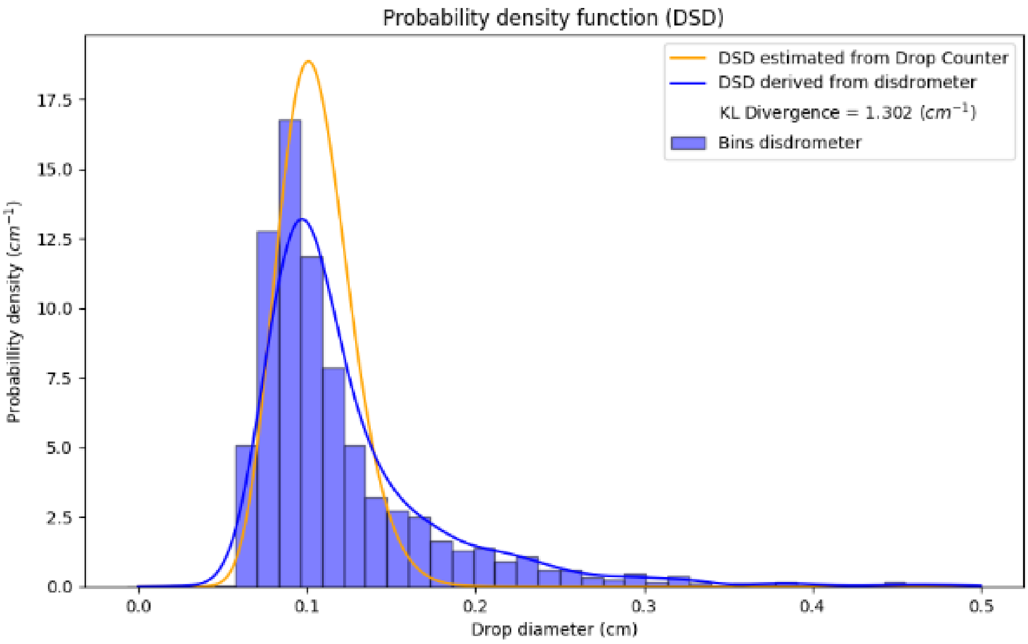

Figure 12: DSD's estimated by DC 2 and Z04 selected from 2017/10/19 8:51 to 2017/10/19 9:22 (grey shaded area in Figure 11).

4.2.1.1 *Sensitivity analysis C_{N_0}*

Since the fit in Figure 12 shows a KL-divergence bigger than 1, a sensitivity analysis is performed similar to the one in section 4.1.3.2. Here the effect of varying C_{N_0} on the KL-divergence of the selected precipitation event from 2017/10/19 8:51 to 2017/10/19 9:22 is assessed. The results of this analysis are presented in Figure 13. It is observed that the best fit is obtained when C_{N_0} is close to 10^4, where C_{N_0} shows a minimum.

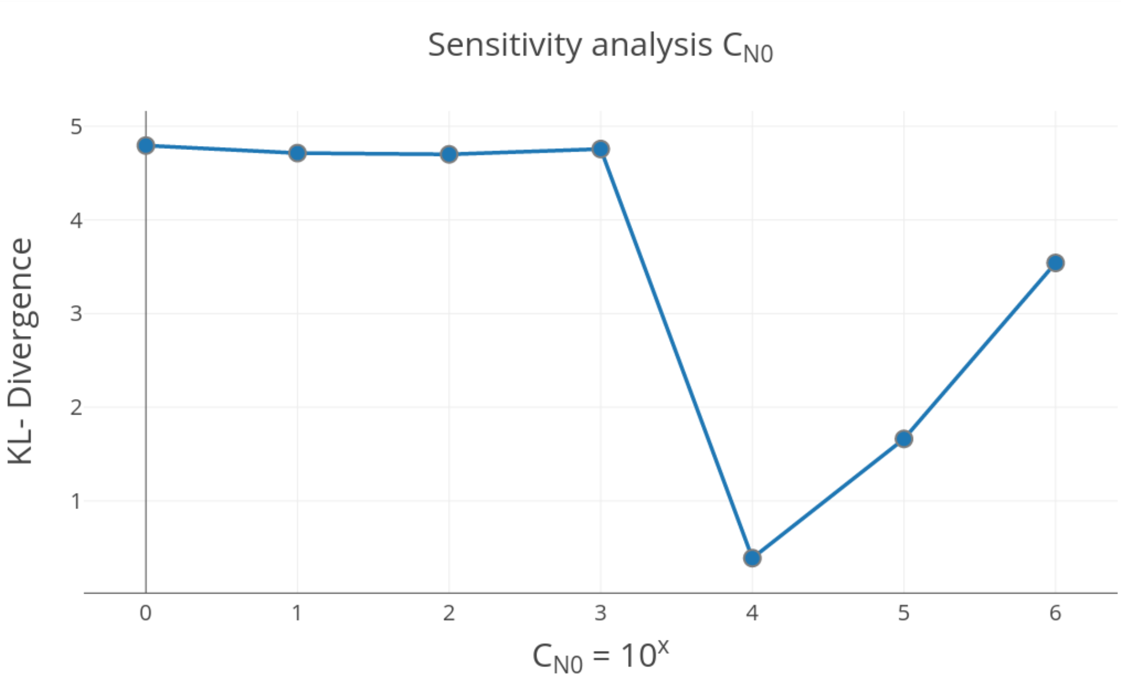

Figure 13: Results of sensitivity analysis C_{N_0} with respect to KL-divergence of DSD of the selected precipitation event from 2017/10/19 8:51 to 2017/10/19 9:22.

5 Discussion

Discussion of the results

5.1 Errors due to wind

Apart from the fact that some of the measurements were lost or damaged due to stormy weather in the winter of 2017/2018 in the Netherlands, very strong winds may cause additional difficulties. The sensitivity of the Drop Counter is optimized in order to maximize the range of detectable drops. In the laboratory it is observed that a strong blow of breath can trigger the piezo (Pape, 2018). Therefore a very strong wind gust can trigger the piezo as well. The error due to strong winds is observed in the dataset of DC 1 and KNMI 1 in Figure 9. In the time period from 18/01/2018 8:00 to 18/01/2018 12:00 high rain intensities are registered by the DC 1, where no or very low intensities are registered by KNMI 1. A zoom of this event is presented in Figure 14. This time period exactly coincides with the times of a passing storm at the Bilt (*KNMI - Code rood voor zeer zware windstoten op 18 januari 2018*, no date). At what wind speeds the piezo is triggered and is hence not showing incoming drops anymore is not investigated in detail. However, it is stated that with a wind force bigger than 9, the results of the Drop Counter lose their reliability.

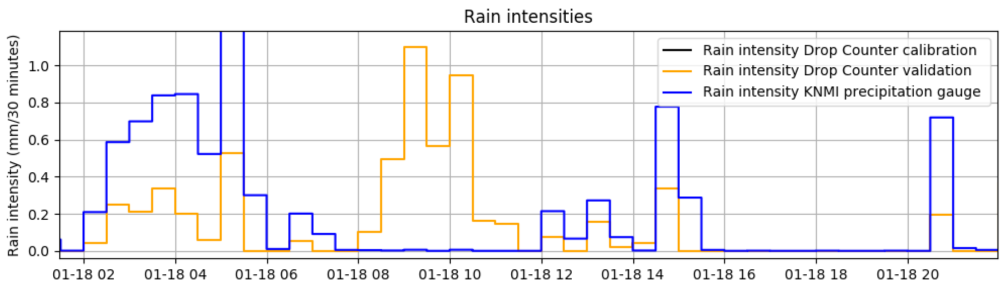

Figure 14: Rain intensity of DC 1 and KNMI 1 from 18/01/2018 3:00 to 18/01/2018 15:00

Note that when the results from 18/01/2018 8:00 to 18/01/2018 12:00 are filtered from the set of DC 1 and KNMI 1, the results significantly increase. The R^2 of the intensity of the rain depth is increased to 0.80 which is a significant improvement of $R^2 = 0.52$ in Table 5. If on top of that C_{N_0} is optimized as well, the results even further increase. The results are visualized in Figure 15 and show an R^2 of the intensity and RMSE of the rain depth of respectively 0.80 and 3.42 mm.

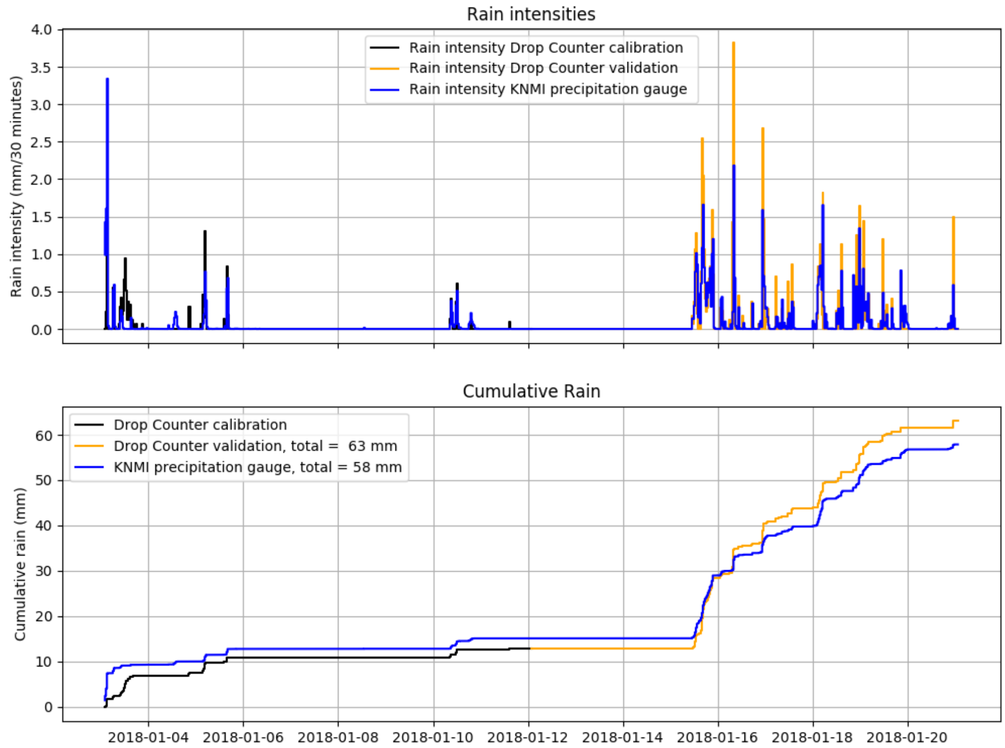

Figure 15: Results DC 1 and KNMI 1, from 03/01/2017 to 23/01/2017 with $C_{N_0} = 10$ and corrected for storm on 18/01/2018 8:00 to 18/01/2018 12:00.

5.2 Results Drop Counter in perspective

In order to put the results from the Drop Counters into perspective, previous work of (Tokay, Bashor and McDowell, 2010) who investigated different rain gauges in the mid-Atlantic is used as a reference. They investigated the performance of rain gauges (mostly tipping buckets) from the NASA TRMM satellite validation office (TSVO) to operational rain gauges at different sites in the mid-Atlantic. Their results are presented in terms of respectively daily average and monthly average errors. It is observed that 75 days of cumulative rainfall had less than a 2% difference between TSVO and Hydrological Services of America (HAS) gauges.

The DC 2 and Z04 sets show that the cumulative rainfall of 14 days measured by DC 2 results in a difference of 1.8% with respect to the Z04 gauge. Note that this regards the calibration and validation set combined so this set is not completely independent. The validation set of DC 2 shows a discrepancy in rain depth of 13.1% over 7 days with respect to Z04.

The results from DC 1 and KNMI 1 with $C_{N_0} = 10$ and corrected for the storm event (like in Figure 15) show that the cumulative rainfall over 18 days result in a discrepancy of 9.1% with respect to KNMI 1. The validation set of DC1 only shows a discrepancy of 17.9% with respect to KNMI 1 for 9 days of measurements. This error is bigger with respect to the set in Myanmar. This is due to two reasons: Firstly the precipitation in Myanmar was more intense, so low rain intensities are not so frequent. Secondly, the disdrometer which is used in the dataset from DC 2 and Z04 has a lower limit for small raindrops as well. Hence the results will coincide more with the results from the Delft disdrometer.

Since the datasets used in (Tokay, Bashor and McDowell, 2010) are much longer than the sets in this work, it is hard to draw any solid conclusions regarding the Drop Counter. However, it is observed that for a shorter validation dataset the Drop Counter shows 6 to 9 times a bigger error as the standardized rain gauges which are considered by (Tokay, Bashor and McDowell, 2010).

5.3 Feedback on theory

If the Drop Counter is actually counting all incoming drops and no noise such as strong wind gusts are registered, the data also provides a feedback on the used relations. First of all, the sensitivity analysis of C_{N_0} shows that the empirical relation $N_0 = C_{N_0} \cdot \exp(C_\mu \cdot \mu)$ with $C_{N_0} = 6.0 \cdot 10^4$ and $C_\mu = 3.14\ cm$ assessed by (Ulbrich, 1983) is not representing the optimal relation for the used data. This is supported by the fact that the statistics of the validation set for DC 1 and KNMI improve when C_{N_0} is decreased. However, note that in the work of (Ulbrich, 1983), μ is assessed per precipitation event and not for an entire dataset. This is supported by the analysis from section 4.2.1.1, where the effect of C_{N_0}on the fit of a DSD of a single precipitation event is analysed. In this analysis C_{N_0} shows a minimum around $1*10^4$ which is close to the suggested value of $1.52*10^4$ by (Ulbrich, 1983). Hence revising the calibration method and assessing a relation between the arrival rate ρ_A and μ might lead to other insights regarding the empirical relations.

Secondly, the DSD measured by the disdrometer in Figure 12 and the distribution estimated by the Drop Counter (with $C_{N_0} = 1 \cdot 10^4$) is showing a relatively good fit for the selected precipitation event. From Figure 13 it is observed that the KL-divergence is 0.31 which is smaller than 1. However, this also means that the theoretical relations sketched in Figure 5 and suggested by (Uijlenhoet and Stricker, 1999) are too simple and do not represent reality. This is supported by the measurements from disdrometer Z04 in Figure 12, where it is observed that the probability of small drops is much lower than Figure 5 suggests. This can partially be due to the fact that the disdrometer has a detection limit for small drops. However, since the probability of bigger drops is also underestimated by the distribution suggested by (Uijlenhoet and Stricker, 1999), it is concluded that this distribution does not represent reality for a monsoon precipitation event. This is supported by the work of (Honingh, 2016) who showed that for DSD's measured in Bago (Myanmar) a generalized gamma fit always (suggested by (Ulbrich, 1983)) outperforms a gamma fit (Uijlenhoet and Stricker, 1999).

5.4 Shortage of data

In this work a short overview is provided on the prospects of the concept of the Drop Counter. Although some datasets already show some promising results regarding the ability of the Drop Counter to estimate the DSD and from that the rain intensity and rain depth, the short datasets make it hard to make any solid statement. According to the WMO guidelines ('www.wmo.int Guide to Meteorological Instruments and Methods of Observation', 2008) any observation should be long enough to guarantee an error in the calculated rain intensity of less than 1%. This condition is not met with the data thus far collected from the Drop Counters. In addition, to guarantee that the calibration and validation set are completely independent it is best to have at least one year of data. An alternative would be to calibrate the Drop Counter at one site and perform a validation at another.

The limited data availability is caused by some malfunctioning in the Drop Counter at the start of the project in Myanmar and the Netherlands. The first design of the Drop Counter was producing erroneous results, which was solved only at the end of the stay. Apart from that, the datasets gathered in the Netherlands are limited by the stormy weather at the end of December 2017 and the 18th of Januray 2018 (*KNMI - Code rood voor zeer zware windstoten op 18 januari 2018*, no date). Consequently the sensor at the KNMI site was blown out of the PVC pipe which made a part of the dataset useless. At the site in Delft the power supply was realised by a combination of a solar panel and a battery. Because the solar panel was blown over, the sensor did not register enough data to analyse any data from this site.

5.5 Recommendations

The following recommendations are made regarding the improvement of the Drop Counter and following research.

- Because a lot of the data was lost due to power shortages or bad weather, the first suggestion is to improve the robustness of the Drop Counter. The rain gauge should be able to operate under extreme weather conditions in terms of temperature, wind speed or precipitation events. This can be realized by making sure the device is anchored in the ground and each compartment (logger box, piezo element etc.) is fixed tightly by using superglue.
- Secondly the power supply of the Drop Counter should be more sustainable. I.e. in the current design a socket is required to supply the logger with power. However, a combination with a battery and a solar panel would make the power supply more sustainable in regions where power supply is unstable or not present.
- The gathering of the data should be simplified. Since the Drop Counter is required to provide in city science, the effort by the user should be minimised. An example of a simplification would be to send the data packages automatically by making use of a long range low battery network (LoRa)(*LoRa | KPN Grootzakelijk*, no date). There are already Arduino-compatible shields which provide LoRa transceiving possibilities. If this innovation is combined with a sustainable power source, the Drop Counter only needs to be installed once and can gather data for at least ten years without demanding any maintenance.
- More data should be gathered in order to perform additional analyses. It would for example be useful to investigate whether μ and the arrival rate ρ_A are related. Consequently an empirical relation can be constructed which could take away the demand for calibration of each Drop Counter. In addition, it is expected to improve the results since each precipitation event has an optimal μ-value.
- A laboratory test should be performed to investigate the wind speeds which are strong enough to trigger the sensor. Hence a threshold can be presented to assess which results are showing the impact of raindrops and which can be considered as noise.

6 Conclusions

Prospects on the use of a Drop Counter

6.1 How accurate can the Drop Counter measure the rain intensity?

It can be concluded that the Drop Counter will not reach the same level of detail as the other rain gauges used in this work. This is due to the implied condition that a minimum number of drops is required to perform a statistical analysis. Therefore the window length is suggested not to be any shorter than 30 minutes. With this integration time and with optimized initial conditions, the rain intensity can be estimated with a RMSE between 0.2 and 0.3 mm. The coefficient of correlation R^2 for the intensity of the investigated datasets ranges from 0.75 to 0.8.

6.2 How accurate can the cumulative rainfall be presented by the Drop Counter compared to other rain gauges?

For the investigated datasets the correlation coefficient R^2 for the rain depth ranges from 0.97 to 0.99, provided that the initial conditions are optimized and the sets are corrected for strong winds. For the full (calibration + validation) datasets differences ranging between 1.8% and 9.1% are observed in the rain depth estimated by the Drop Counter and measured by reference gauges. Compared to errors between two WMO standard gauges (Tipping Buckets) these errors are respectively in the same order of magnitude and 5 times as big.

6.3 Do the DSD's estimated by the Drop Counter correspond to the DSD's measured by another rain gauge?

The KL-divergence is set as a standard for the correspondence of the estimated DSD by the Drop Counter with respect to a reference gauge. The fit of the DSD is very dependent of each precipitation event. For an example precipitation event in Myanmar, the KL-divergence was shown to range from 0.3 cm^{-1} to 4.8 cm^{-1}. The lower and upper limits showing respectively the results for unoptimized and optimized C_{N_0}-values. KL-divergences lower than 1 cm^{-1} were defined as a good fit. Hence the DSD's estimated by the Drop Counter correspond well to the DSD's measured by reference rain gauges, provided that C_{N_0} is optimized.

6.4 Theory revisited

The feedback provided by the Drop Counter shows that the theoretical relations for the DSD assed by (Ulbrich, 1983) are applicable on a single precipitation event. However, when a period of multiple precipitation events is considered, the relations do not lead to optimal results. Apart from that, the measurements from the Delft disdrometer show that one parameter Λ which determines the DSD, suggested by (Uijlenhoet and Stricker, 1999), is a too simple approximation for a monsoon precipitation event.

6.5 General conclusion

Since the Drop Counter is cheap (total costs should not exceed $40,- per device) and made of material which are worldwide available, at least two of the three conditions on the aims of the Drop Counter are met. The third aim is to provide the user of useful rainfall data. It can be concluded that the estimated rain intensities and rain depth are highly ($R^2 > 0.75\ and > 0.98$ respectively) correlated to reference gauges. The errors in the rain depth are relatively high compared to WMO standards, but since the datasets are short this is expected to improve. On top of that, the results are obtained in two climates which supports the compatibility of the Drop Counter worldwide. Therefore the ability of the Drop Counter to estimate rain related parameters is concluded to be good and the potential of this simple device in urban water management is high.

7 References

Arduino - Knock sensor (no date). Available at: https://www.arduino.cc/en/Tutorial/Knock (Accessed: 12 December 2017).

Brent, R. (2013) 'Algorithms for minimization without derivatives'. Available at: https://books.google.nl/books?hl=nl&lr=&id=AITCAgAAQBAJ&oi=fnd&pg=PP1&dq=Algorithms+for+Minimization+Without+Derivatives+brent&ots=p37xFbB33x&sig=kzyB5Xh3BzpAckEU9Eko7TgETaY (Accessed: 10 January 2018).

Girons lopez, M. *et al.* (2015) 'Location and density of rain gauges for the estimation of spatial varying precipitation', *Geografiska Annaler: Series A, Physical Geography*, 97(1), pp. 167–179. doi: 10.1111/geoa.12094.

Honingh, D. F. (2016) *Global Precipitation Measurement data compared to ground based disdrometer measurements,*. TU Delft.

Hut, R. *et al.* (2013) 'Design and field test of a robust acoustic disdrometer for distributed rainfall observations', *EGU General Assembly 2013, held 7-12 April, 2013 in Vienna, Austria, id. EGU2013-12388*, 15. Available at: http://adsabs.harvard.edu/abs/2013EGUGA..1512388H (Accessed: 11 December 2017).

KNMI (no date) *KNMI - Meer regen meten in steden*. Available at: https://www.knmi.nl/over-het-knmi/nieuws/meer-regen-meten-in-steden (Accessed: 11 December 2017).

KNMI - Code rood voor zeer zware windstoten op 18 januari 2018 (no date). Available at: http://www.knmi.nl/kennis-en-datacentrum/achtergrond/code-rood-voor-zeer-zware-windstoten-op-18-januari-2018 (Accessed: 26 January 2018).

Kottek, M. *et al.* (2006) 'World Map of the Köppen-Geiger climate classification updated', *Meteorologische Zeitschrift*, 15(3), pp. 259–263. doi: 10.1127/0941-2948/2006/0130.

Kullback, S. and Leibler, R. A. (no date) 'On Information and Sufficiency', *The Annals of Mathematical Statistics*. Institute of Mathematical Statistics, pp. 79–86. doi: 10.2307/2236703.

Llasat, M.-C. (2001) 'An objective classification of rainfall events on the basis of their convective features: application to rainfall intensity in the northeast of spain', *International Journal of Climatology*, 21(11), pp. 1385–1400. doi: 10.1002/joc.692.

LoRa | KPN Grootzakelijk (no date). Available at: https://www.kpn.com/zakelijk/grootzakelijk/internet-of-things/lora-netwerk.htm (Accessed: 26 January 2018).

Marshall, J. S. *et al.* (1948) 'THE DISTRIBUTION OF RAINDROPS WITH SIZE', *Journal of Meteorology*, 5(4), pp. 165–166. doi: 10.1175/1520-0469(1948)005<0165:TDORWS>2.0.CO;2.

Mesas-Carrascosa, F. J. *et al.* (2015) 'Open source hardware to monitor environmental parameters in precision agriculture', *Biosystems Engineering*. Academic Press, 137, pp. 73–83. doi: 10.1016/J.BIOSYSTEMSENG.2015.07.005.

Muller, C. L. *et al.* (2015) 'Crowdsourcing for climate and atmospheric sciences: current status and future potential', *International Journal of Climatology*, 35(11), pp. 3185–3203. doi: 10.1002/joc.4210.

Pape, J. J. (2018) *Logbook Drop Counter*. Utrecht.

Rodda, J. C. (2011) 'Guide to Hydrological Practices', *Hydrological Sciences Journal*, 56(1), pp. 196–197. doi: 10.1080/02626667.2011.546602.

van het Schip, T. I. *et al.* (2017) 'Rainfall measurement using cell phone links: classification of wet and dry periods using geostationary satellites', *Hydrological Sciences Journal*, 62(9), pp. 1343–1353. doi: 10.1080/02626667.2017.1329588.

Scott, D. (2015) 'Multivariate density estimation: theory, practice, and visualization'. Available at:

https://books.google.nl/books?hl=nl&lr=&id=XZ03BwAAQBAJ&oi=fnd&pg=PA242&dq=D.W.+Scott,+‘Multivariate+Density+Estimation:+Theory,+Practice,+and+Visualization’,+John+Wiley+%26+Sons,+New+York,+Chicester,+1992.&ots=jAR-vGpupw&sig=c9RKgVXqELTcE29fT9GUFIet8d0 (Accessed: 23 January 2018).

Tokay, A., Bashor, P. G. and McDowell, V. L. (2010) ‘Comparison of Rain Gauge Measurements in the Mid-Atlantic Region’, *Journal of Hydrometeorology*, 11(2), pp. 553–565. doi: 10.1175/2009JHM1137.1.

Uijlenhoet, R. and Stricker, J. N. M. (1999) ‘A consistent rainfall parameterization based on the exponential raindrop size distribution’, *Journal of Hydrology*, pp. 101–127. doi: 10.1016/S0022-1694(99)00032-3.

Ulbrich, C. W. (1983) ‘Natural Variations in the Analytical Form of the Raindrop Size Distribution’, *Journal of Climate and Applied Meteorology*, 22(10), pp. 1764–1775. doi: 10.1175/1520-0450(1983)022<1764:NVITAF>2.0.CO;2.

‘www.wmo.int Guide to Meteorological Instruments and Methods of Observation’ (2008). Available at: https://library.wmo.int/pmb_ged/wmo_8_en-2012.pdf (Accessed: 25 January 2018).